ARTICLES SCIENCE CHINA Materials

mater.scichina.com link.springer.com

Published online 16 December 2019 | https://doi.org/10.1007/s40843-019-1218-1

Sci China Mater 2020, 63(3): 364–374

First principles study on methane reforming over $Ni/TiO_2(110)$ surface in solid oxide fuel cells under dry and wet atmospheres

Wenqiang Yang[1], Zhenbin Wang[1], Wenzhou Tan[1], Ranran Peng[1*], Xiaojun Wu[1,2,3*] and Yalin Lu[1,2,3*]

ABSTRACT **Understanding the carbon-tolerant mechanisms from a microscopic view is of special importance to develop proper anodes for solid oxide fuel cells. In this work, we employed density-functional theory calculations to study the CH_4 reaction mechanism over a Ni/TiO_2 nanostructure, which experimentally demonstrated good carbon tolerance. Six potential pathways for methane reforming reactions were studied over the $Ni/TiO_2(110)$ surface under both dry and wet atmospheres, and the main concerns were focused on the impact of TiO_2 and Ni/TiO_2 interface on CO/H_2 formation. Our calculations suggest that the reaction between carbon and the interfacial lattice oxygen to form CO* is the dominant pathway for CH_4 reforming under both dry and wet atmospheres, and intervention of steam directly to oxidize C* with its dissociated OH* group is less favorable in energy than that to wipe off oxygen vacancy to get ready for next C* oxidation. In all investigated paths, desorption of CO* is one of the most difficult steps. Fortunately, CO* desorption can be greatly promoted by the large heat released from the previous CO* formation process under wet atmosphere. H_2O adsorption and dissociation over the TiO_2 surface are found to be much easier than those over Ni, yttria stabilized zirconia (YSZ) and CeO_2, which should be the key reason for the greatly depressed carbon deposition over $Ni-TiO_2$ particles than traditional YSZ-Ni and CeO_2-Ni anode. Our study presents the detailed CO* formation mechanism in CH_4 reforming process over the Ni/TiO_2 surface, which will benefit future research for exploring new carbon-tolerant solid oxide fuel cell anodes.**

Keywords: solid oxide fuel cells, carbon tolerance, methane reforming, first principles

INTRODUCTION

Driven by the global concerns on environment pollution and energy crisis, intermediate temperature solid-oxide fuel cells (IT-SOFCs) have drawn special attention due to their high energy conversion efficiency, low toxic gas emission and great fuel flexibility [1]. Unfortunately, when directly used in hydrocarbon fuels, such as methane and propane, severe carbon formation over the traditional Ni-based anodes (e.g., Ni-YSZ (yttria stabilized zirconia) and Ni-SDC (Sm-doped ceria) anodes) occurs which leads to dramatical performance degradation and sometimes the cell cracking [2]. Therefore, numerous studies have been proposed to alleviate this problem [3] in the past decades, including 1) substituting Cu and other transition metals that have low activity toward hydrocarbon fuel cracking for Ni catalysts [3–7]; 2) developing new carbon-tolerant oxide anode materials, such as $La_{0.75}Sr_{0.25}Cr_{0.5}Mn_{0.5}O_{3-\delta}$ (LSCM) [8,9], $SrTiO_3$ (STO) [10,11], $Sr_2Fe_{1.5}Mo_{0.5}O_{6-\delta}$ (SFM) [12,13] and $Pr_{0.4}Sr_{0.6}Co_{0.2}Fe_{0.7}Nb_{0.1}O_{3-\delta}$ (PSCFN) [14]; and 3) microstructure optimization of traditional Ni-based anodes using CeO_2 [15] or BaO [16] nano-particles. The above methods are effective in improving the anode carbon tolerance when used in hydrocarbon fuels. However, they usually bring forth other problems, such as the depressed cell electrochemical properties [7,9], the high operating temperatures required [9–15] and the increased fabrication cost [16,17].

Recently, Shinde *et al.* [18] found that the Ni/TiO_2 catalyst had a high resistance to coke formation even at a low steam/carbon ratio, much better than the traditional

[1] CAS Key Laboratory of Materials for Energy Conversion, Department of Materials Science and Engineering, University of Science and Technology of China, Hefei 230026, China
[2] Hefei National Laboratory of Physical Science at the Microscale, University of Science and Technology of China, Hefei 230026, China
[3] Synergetic Innovation Center of Quantum Information & Quantum Physics, University of Science and Technology of China, Hefei 230026, China
* Corresponding authors (emails: pengrr@ustc.edu.cn (Peng R); xjwu@ustc.edu.cn (Wu X); yllu@ustc.edu.cn (Lu Y))

Ni/ZrO_2 catalysts (about 59% C selectivity) [19]. We also found that single cells demonstrated great power density and stability in methane and propane atmospheres when applying a Ni-TiO_2 catalytic layer *in-situ* formed *via* Ni-TiO_3 reduction [20,21]. Compared with the traditional Ni-YSZ and Ni-SDC catalysts that generally facilitate the coke forming reaction, the great carbon tolerance of the Ni/TiO_2-based catalysts should result from the special properties of TiO_2 or the Ni/TiO_2 interface. Unfortunately, so far a detailed mechanism of the promoted carbon formation resistance of such materials in hydrocarbon atmosphere and especially the role of TiO_2 in the coke removing reactions are still unclear. Particularly, the absence of an atomistic level understanding on the improved carbon tolerance mechanism brings no clues on how to effectively explore advanced carbon-tolerant anodes.

First-principles calculations based on density functional theory (DFT) have been demonstrated as a powerful tool to give atomic insights into the methane decomposition and reforming reaction mechanisms. So far, these investigations were mainly focused on the catalytic activity of noble or transition metals, including Ni [4,22–24], Pt [25], Pd [26,27] and Ru [28,29], while much less efforts are on that of the metal/oxide interfaces. In this work, based on the DFT, CO and H_2 formation from methane reforming and oxidizing over the $Ni/TiO_2(110)$ surface were systematically investigated under both dry and wet atmospheres, with a goal to get a comprehensive understanding of the role of TiO_2 and Ni/TiO_2 interface in the methane reforming reactions. Notably, carbon deposition is extremely severe under open circuit conditions where no oxygen ions are transferred from the cathode to anode. And thus, herein the reactions of CH_4 with lattice oxygen of TiO_2 under dry atmosphere, and with both lattice oxygen and adsorbed H_2O under wet atmosphere were mainly focused on. The dominant processes and the most difficult steps were determined for both dry and wet CH_4 oxidizing and reforming reactions. Steam adsorptions over TiO_2, YSZ and CeO_2 were also calculated to declare their differences toward CH_4 reforming reactions.

COMPUTATIONAL METHOD

All calculations were conducted based on the DFT with the projector augmented wave method [30], and accomplished by Vienna *ab initio* simulation package [31,32]. In treating the exchange correlation effect, the generalized gradient approximation (GGA) with the Perdew-Burke-Ernzerhof (PBE) functional [33] was used. The kinetic energy cutoff was set as 420 eV and the energy convergence criterion was 10^{-6} eV per atom. For the structure optimization, all structures were relaxed until the Hellmann-Feynman force on each atom was smaller than 0.03 eV $Å^{-1}$. All calculations were spin-polarized. We adopted a 2×2×1 k-points mesh using the Monkhorst-Pack method to sample the integration in Brillouin zone [34]. Meanwhile, the location and the energy of the transition states were calculated using the climbing image nudged elastic band (CI-NEB) method [35].

It is well known that rutile phase TiO_2 (r-TiO_2) is the most stable phase under the realistic SOFC experimental conditions [36] and r-$TiO_2(110)$ surface plays an active role in many reactions, such as photocatalysis and water-gas shift reactions [37–40]. Hence, r-$TiO_2(110)$ surface was adopted in our calculations. A 4×2 (110) surface slab model with four tri-layers (containing 128 oxygen atoms and 64 titanium atoms) was built for our calculations, as shown in Fig. 1. Test calculations of a larger 5×2 surface slab present similar surface energy and oxygen vacancy formation energy with that of the 4×2 surface slab, and the difference in energy is less than 0.1 eV. A 15 Å va-

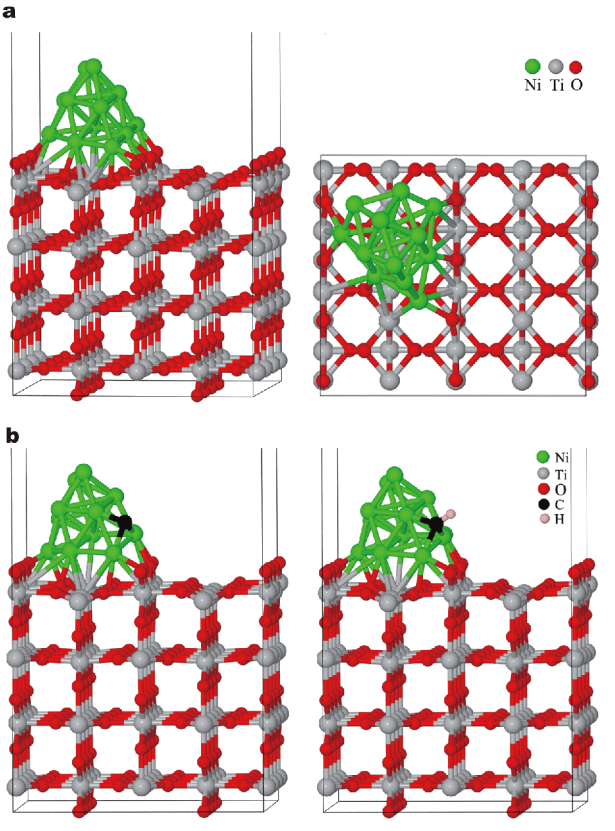

Figure 1 (a) The side and top view of the $Ni_{13}/TiO_2(110)$ surface slab and (b) the optimized structures of C and CH adsorbed $Ni_{13}/TiO_2(110)$ surface.

cuum space was built to separate the periodic surface slab and to avoid the interactions between periodic surface slabs. For all surface calculations, the bottom two tri-layers' atoms were fixed at their bulk positions with the top two tri-layers fully relaxed. A three-layer Ni cluster containing 13 atoms (Ni_{13}) [41] was constructed on the r-TiO_2(110) surface to simulate the Ni/TiO_2 nano-particle, as displayed in Fig. 1a.

RESULTS

It is known that there are four steps in methane dissociation to surface CH* and C* species, as expressed in Equations (1–4), which are very fast on transition metal surfaces, such as Ni, Ru and Pt [42–45]. Thus, the reactions of C* and CH* with surface oxygen or OH* to form CO and H_2 are mainly considered here to find out how H_2O and TiO_2 are involved in the steam reforming or oxidizing reactions of methane [2–4,18,24] as expressed in Equations (5–8):

$$CH_4 + 2* \rightarrow CH_3* + H*, \quad (1)$$

$$CH_3* + * \rightarrow CH_2* + H*, \quad (2)$$

$$CH_2* + * \rightarrow CH* + H*, \quad (3)$$

$$CH* + * \rightarrow C* + H*, \quad (4)$$

$$C* + O* \rightarrow CO* + *, \quad (5)$$

$$C* + OH* \rightarrow COH* + *, \quad (6)$$

$$CH* + O* \rightarrow CHO* + *, \quad (7)$$

$$CH* + OH* \rightarrow CHOH* + *, \quad (8)$$

where * denotes an active free surface site and M* (M=CH_3, CH_2, CH, C, O, OH, CHO and CHOH) denotes a surface species M. Here, O* and OH* may form *via* the steam dissociation or the lattice oxygen releasing. The optimized stable structures of C and CH adsorption on the Ni_{13}/TiO_2(110) surface are shown in Fig. 1b, where both C and CH prefer to adsorb on the Ni/TiO_2 interfacial sites, indicating a probable active role of the interfacial sites. Starting from C* and CH* surface species, six possible reaction pathways, named as C-O, C-O-steam, C-OH-steam, CH-O, CH-O-steam and CH-OH-steam paths, were proposed to illustrate the formation of CO and H_2 under dry and wet atmospheres (with and without steam involved), as shown in Fig. 2. In these path names, C and CH denote the reaction starting from C* and CH*, respectively; O and OH denote surface oxygen O* and hydroxyl OH* involved in the oxidization of CH and C, respectively; and steam indicates the wet atmosphere. For example, C-O path indicates that the reaction

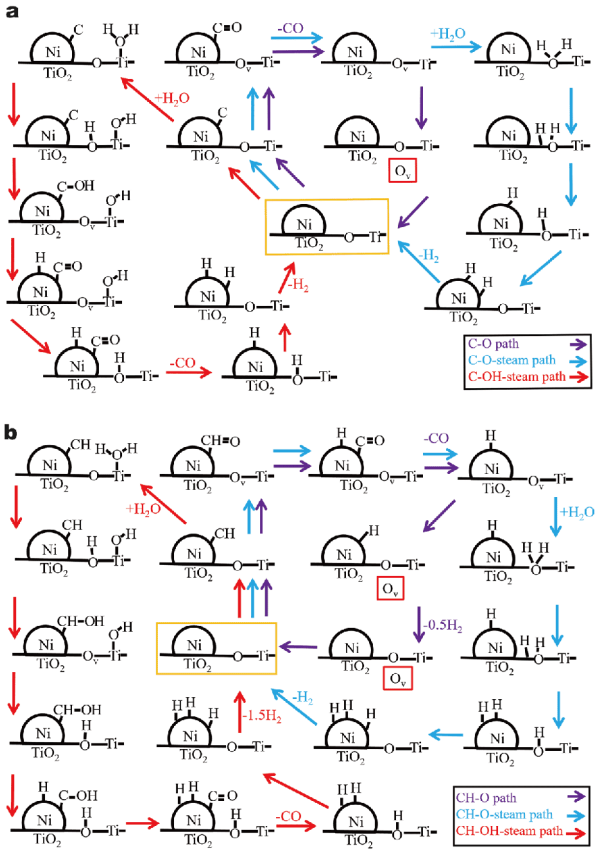

Figure 2 Reaction pathways of possible CO (a) and H_2 (b) formation with and without the assistance of steam on the Ni_{13}/TiO_2(110) surface, where O_v and orange rectangular denote oxygen vacancy and the origin clean surface, respectively.

path starts with C* and C* is oxidized by surface O* under dry atmosphere; and C-OH-steam path indicates that the reaction path starts with C* and C* is oxidized by surface OH* under wet atmosphere.

Under dry atmosphere

C-O path

Firstly, the adsorbed C* reacts with the interfacial lattice oxygen from TiO_2, forming CO* on the interfacial site and leaving an oxygen vacancy at the interfacial region, and then the formed CO* desorbs from the solid surface (purple arrow indicated in Fig. 2a). As shown in Fig. 3, the formation of CO* (S2 to S11) needs to overcome an energy barrier of 1.30 eV and releases 0.82 eV of heat. However, the desorption of CO* (S11 to S12) is greatly endothermic (2.1 eV) without energy barrier, implying that the adsorption of CO is thermodynamically stable on the surface, and that the active interfacial sites may be

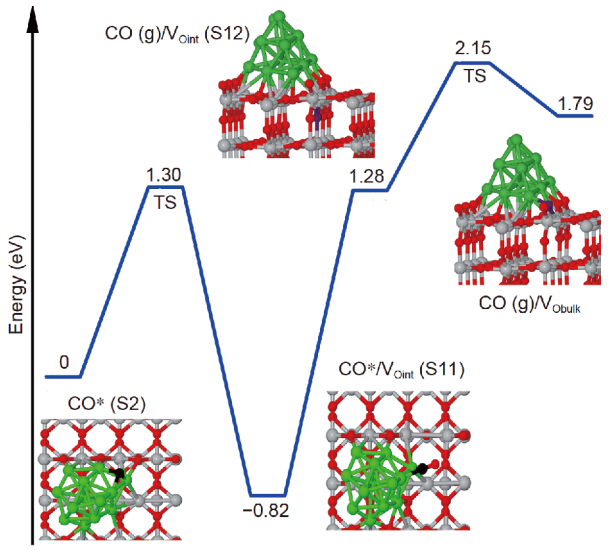

Figure 3 Illustration of the C-O path for carbon removing under dry atmosphere. The purple balls denote the oxygen migration from TiO_2 bulk to the surface. V_{Oint} and V_{Obulk} denote the oxygen vacancy at the Ni/TiO_2 interface and TiO_2 bulk, respectively.

blocked and deactivated due to the stable CO adsorption. It can be concluded, therefore, the formation of CO in C-O path is very difficult due to the huge energy needed for CO* desorption, which will result in a deactivated surface for C* oxidation and thus a C* deposited surface.

CH-O path

The adsorbed CH reacts with the bridge lattice oxygen to form CO and H_2, which includes three major steps of the formation of CHO* from CH* and interface lattice O, the dissociation of CHO* to CO* and H*, and the desorption of CO* to gas atmosphere (purple arrow indicated in Fig. 2b). As shown in Fig. 4, unlike the formation of CO* in C-O path, the formation of CHO* (S17 to S26) is endothermic with a heat of 0.97 eV needed. Although the dissociation of CHO* (S26 to S27) into CO* is exothermic (−0.98 eV), the desorption of CO* from the surface into gas phase (S27 to S28) is still very difficult with the energy needed of 2.33 eV. Comparing the energy changes in the C-O path and CH-O path (Figs 3 and 4), it can be found that the CH-O path is even more energetically unfavorable than C-O path under dry atmosphere. It should be also noted that in both paths, the migration of lattice oxygen from bulk TiO_2 to the oxygen vacancy should also be considered for sustainable reaction. Yet, this migration process is also endothermic (about 0.51 eV) and needs to overcome an energy barrier of 0.88 eV. The high energy barrier compared with those of YSZ and CeO_2 which are around 0.28 and 0.50 eV, respectively, implies that the sluggish migration of lattice oxygen to oxygen vacancy cannot effectively accelerate the carbon elimination under dry atmosphere. Considering the large reaction heats needed in the two oxidizing processes under dry atmosphere, we can conclude that both paths are thermodynamically unfavorable and can barely happen, which is consistent with the experimental observation of carbon deposition on Ni-TiO_2

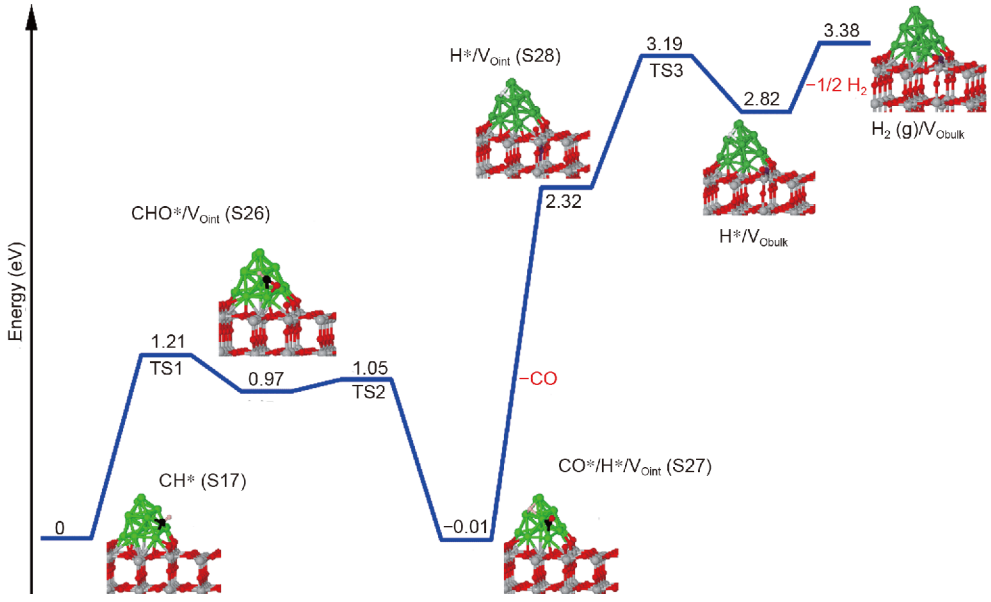

Figure 4 Illustration of CH-O path under dry atmosphere (TS: transition state).

catalysts under dry atmosphere.

Under wet atmosphere

C-O-steam path

Under wet atmosphere, C* may be oxidized by lattice oxygen (C-O-steam path) or directly reformed by steam (C-OH-steam path). In the C-O-steam path (blue arrow in Fig. 2a), the formation and desorption of CO is similar to that of C-O path, and then steam is adsorbed and dissociated over TiO_2 surface to compensate the formed oxygen vacancy (instead of oxygen migration in C-O path). As shown in Fig. 5, after CO desorption, H_2O adsorbs on the oxygen vacancy, which is an exothermic process with an energy release of 0.96 eV. Importantly, the dissociation of H_2O* into two OH* species (S13 and S14) and the following dissociation of OH* (S14 to S16) both intensively release the reaction heat, in spite of their energy barriers (~1 eV) needed to overcome. Compared with C-O path, the processes in C-O-steam significantly reduce the reaction heat of the whole reaction from 1.79 to 0.60 eV, making the whole reaction much more favorable in thermodynamics.

C-OH-steam path

As shown in Fig. 6, prior to the formation of CO*, H_2O adsorbs on the surface Ti site (S1 to S2), which then dissociates with one H* over the interfacial O and the OH* on the TiO_2 surface, releasing 0.84 eV of heat (S3 to S4). Thereafter, C* reacts directly with the interfacial OH*, forming COH* on the Ni_{13} cluster (S4 to S5) and one interfacial oxygen vacancy simultaneously. A large energy barrier as high as 1.83 eV is needed to overcome to fulfill this process. In the following, COH* dissociates into CO* and H* (S5 to S6) with a large amount of heat (about 1.17 eV) released to the environment. The nearby OH* on TiO_2 surface incorporates into the oxygen vacancy with an energy barrier of 0.66 eV, which is lower than the migration energy barrier of lattice oxygen (Fig. S1), and releases 0.89 eV of heat (S6 to S7). Desorption of CO* from the Ni_{13} cluster surface (S7 to S8) is still the hardest one, requiring an extra heat of 2.27 eV. What's the worse, the following migration of H from the interfacial region to Ni_{13} cluster needs to overcome an energy barrier of 1.2 eV

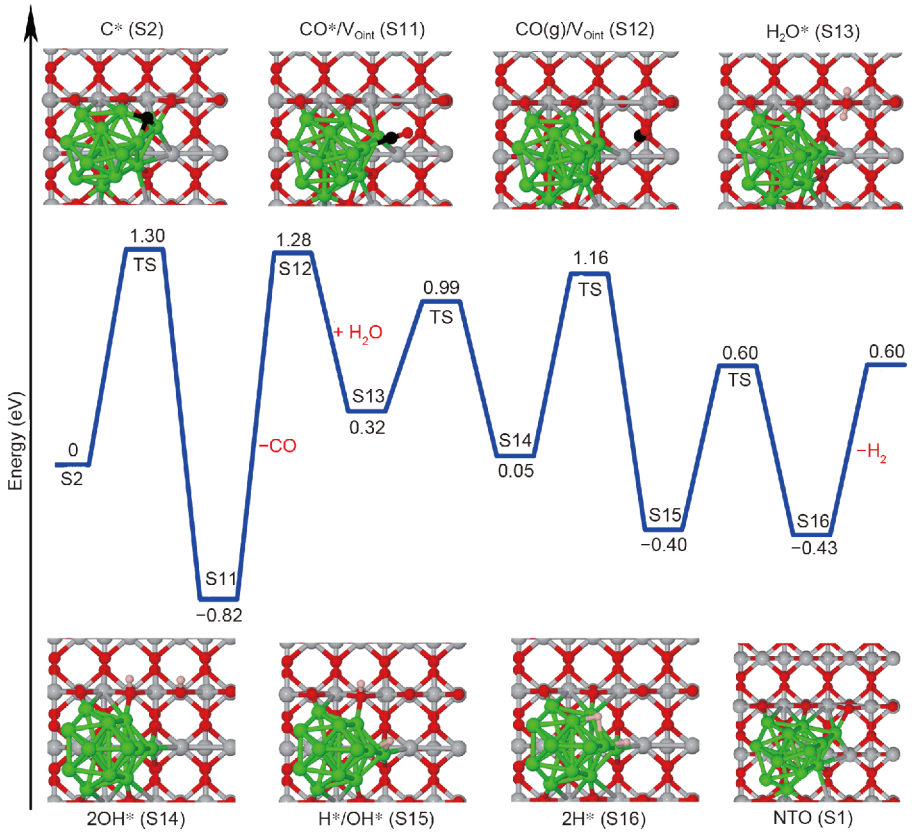

Figure 5 Illustration of C-O-steam path in the presence of H_2O (NTO: Ni_{13}/TiO_2).

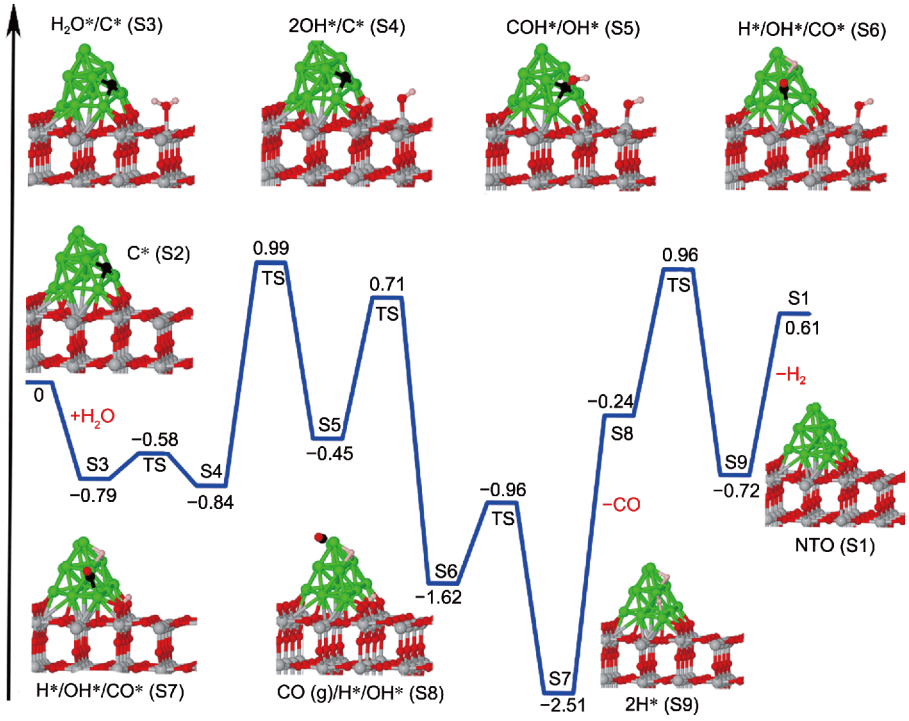

Figure 6 Illustration of the C-OH-steam path in the presence of H_2O.

(S8 to S9), which makes a total 3.47 eV of heat needed to fulfill the process from S7 to S9. Such a large energy requirement along with that for COH* formation indicates that the elimination of adsorbed C* over the Ni/TiO_2 surface under wet atmosphere is more prone to happen through C-O-steam path instead of C-OH-steam path.

CH-O-stem path

Like that of C*, oxidation by lattice oxygen and steam reforming reaction can also occur on CH*. Fig. 7 displays the energy diagram of CH* oxidized by lattice oxygen under wet atmosphere, noted as CH-O-stem path. The first steps (S17 to S28) are the same as that in the CH-O path, in which the CO* desorption is still the most difficult step to occur with a large energy barrier of 2.33 eV. After desorption of CO*, H_2O adsorbs on the oxygen vacancy, releasing 0.82 eV of heat (S28 to S29) to the environment, and then dissociates into two OH* at the interfacial region by overcoming an energy barrier of 0.62 eV (S29 to S30). The two interfacial H* consecutively transfer to nearby Ni sites (S30 → S31 → S32), and finally, desorbs from the surface forming gas phase H_2. Considering that the reaction heat of the whole reaction reduces from 3.38 eV in CH-O path under dry atmosphere to 1.85 eV here in the CH-O-steam path, the existence of H_2O makes the whole reaction much less endothermic and more favorable in thermodynamics. Nevertheless, compared with the energy profile for C-O-steam path in which the CO desorption heat can be largely compensated by that from CO* formation (Fig. 5), it seems that the CH-O-steam path is still less energetically favorable. In other words, direct oxidizing reaction is more prone to happen on C*, instead of CH*.

CH-OH-steam path

As shown in Fig. 8, reaction begins with steam adsorption and dissociation, releasing 0.65 eV of heat in total. CH* then reacts with the interfacial OH* and forms CHOH* species on the Ni_{13} cluster and an oxygen vacancy (S19 to S20), encountering a large energy barrier of 1.82 eV. The other OH* migrates to the oxygen vacancy (S20 to S21), releasing 0.92 eV of heat. In the following, two steps of CHOH* dissociation (CHOH* + * → COH* + H* → CO* + 2H*) occur with energy barriers of 0.79 and 0.43 eV, respectively. Finally, interfacial H atom spills over to the Ni_{13} cluster (S24 to S25). Similar to the other pathways, desorption of CO* from the Ni_{13} cluster (S23 to S24) is still endothermic which needs 2.35 eV energy and is aggravated by the large energy barrier of 1.18 eV for the H spilling over step. Such huge energy demands make

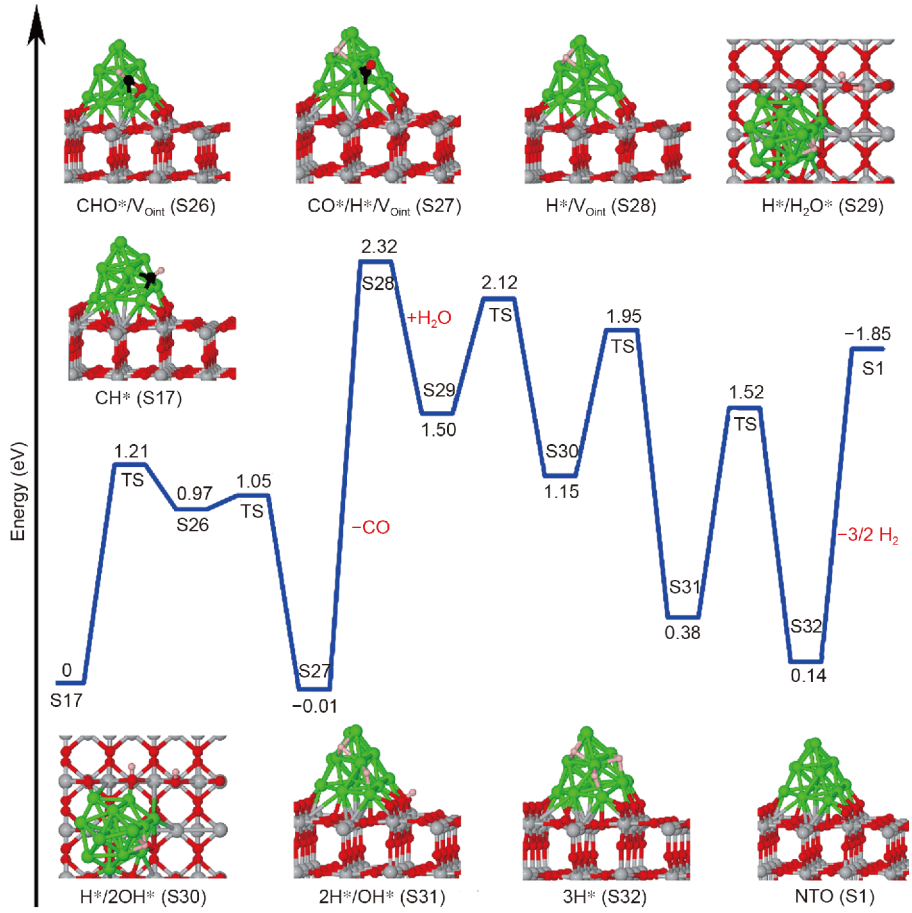

Figure 7 Illustration of the CH-O-steam path in the presence of H_2O.

this pathway difficult to occur, especially considering the strong endothermic formation of CHOH* at the interfacial region which needs to overcome a high energy barrier (1.82 eV). It should be noted that the dissociation of CHOH* is a significantly exothermic reaction with a reaction energy of −1.34 eV, which can partially compensate the energy need of the following CO* desorption step and thus makes CO desorption easier than that uner dry atmosphere (CH-O path). Other possibility of CH-OH-steam and CH-O-steam pathways are also considered and shown in Figs S2 and S3, respectively.

DISCUSSION

Energetically favorable path

Comparing the six possible pathways above for CO and H_2 formation in methane reactions under both dry and wet atmospheres on the Ni/TiO_2(110) surface, it is clear that 1) the direct reaction of the adsorbed C with the bridge lattice O of TiO_2 at the interfacial region is the dominating pathway for the formation of CO* (C-O path and C-O-steam path), demonstrating the active role of lattice O for C* elimination [37–40,46,47]; 2) intervention of steam directly to oxidize C*/CH* with its dissociated OH* group is less favorable in energy than to wipe off oxygen vacancy to get ready for the next C*/CH* oxidation; 3) the filling of oxygen vacancy through steam adsorption is much energetically superior to that through the migration of oxygen ion in bulk TiO_2, and thus accelerates the whole carbon elimination reaction in thermodynamics; 4) the adsorption of H_2O greatly reduces the energy of the system and makes the whole reaction much more favorable in energy than that under dry atmosphere; and 5) CO* desorption is the largest endothermic step, and therefore may greatly impede the whole reaction. The most possible reactions of CO formation over Ni/TiO_2 surface are illustrated in Fig. 9 under dry and wet atmospheres, respectively, where E_a and E_{rxn} denote the reaction energy barriers and the reaction heat, respectively.

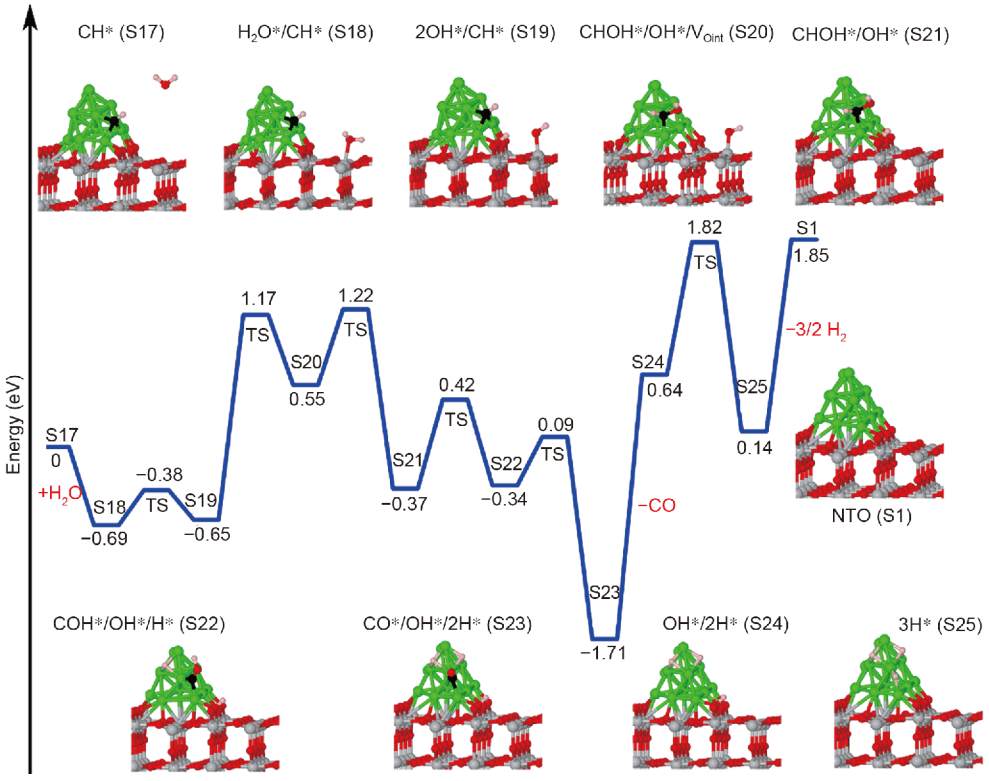

Figure 8 The reaction path of the CH-OH-steam path for the C removing with the assistance of H_2O.

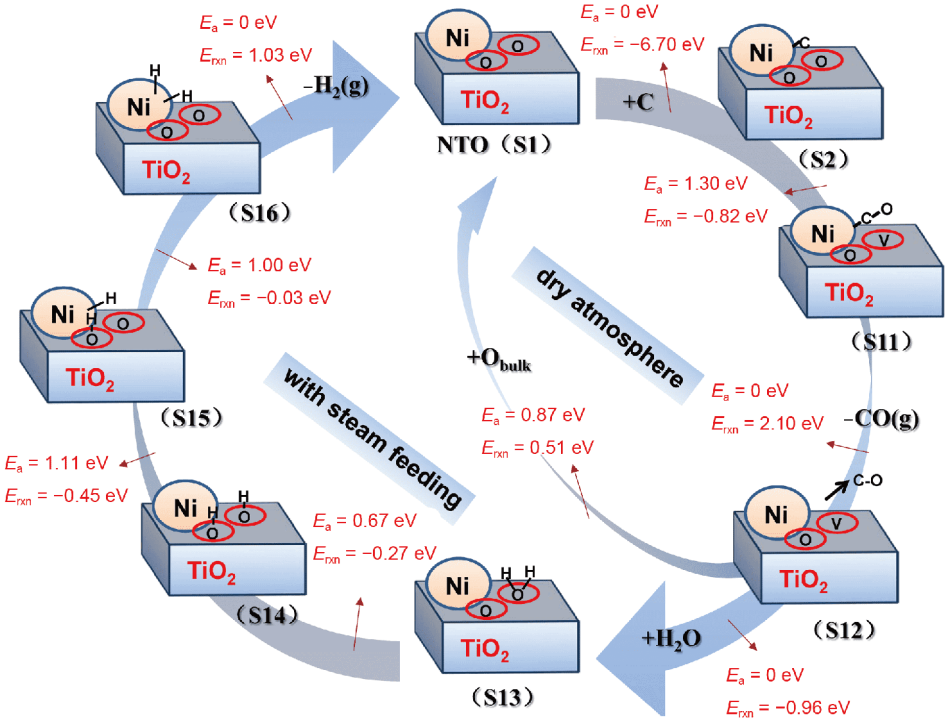

Figure 9 Schematic energy profiles of the C-O path and C-O-steam path.

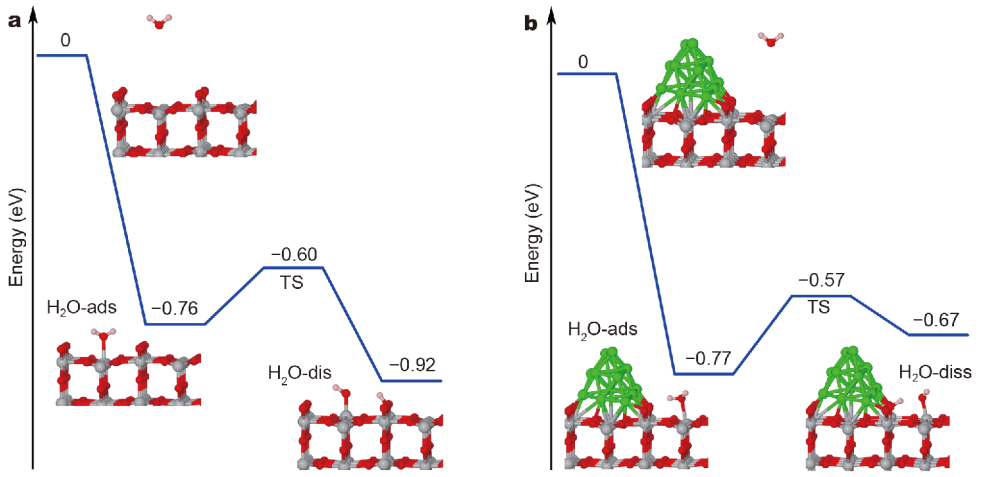

Figure 10 H_2O adsorption and dissociation on the (a) TiO_2(110) and (b) Ni_{13}/TiO_2(110) perfect surfaces, respectively.

Table1 Summary of H_2O adsorption and dissociation on different materials' surfaces with E_{ads} and E_{diss} denoting the adsorption energy and dissociation barriers, respectively

Materials	E_{ads} (eV)	E_{diss} (eV)	Ref.
TiO_2-perfect	−0.76	0.16	This work
Ni_{13}/TiO_2-perfect	−0.77	0.20	This work
Ni_{13}/TiO_2-defect 1 (C-O-steam path)	−0.96	0.67	This work
Ni_{13}/TiO_2-defect 2 (CH-O-stem path)	−0.82	0.62	This work
Ni(111)	−0.02, −0.18, −0.25	0.92	[42,44,48]
YSZ	−0.26	-	[21]
CeO_2	−0.33–−0.56	2.35	[49]

Role of TiO_2 in the formation of CO and H_2

From the above discussion, it is found that TiO_2 plays an active role in H_2O adsorption and dissociation reactions, and thus affects the whole CH_4 reforming reactions. In order to find out details about the role of TiO_2 in the whole reaction processes, the dissociation of H_2O on the perfect TiO_2(110) surface is further considered. As shown in Fig. 10, the adsorption of H_2O on the perfect TiO_2 is spontaneously and exothermic with energy release of 0.76 eV. The adsorbed H_2O transfers one H to the neighboring oxygen, forming two OH* by overcoming a small energy barrier of 0.16 eV. These results highly indicate a fast adsorption and dissociation rate of steam over the TiO_2(110) surface. In addition, the adsorption and dissociation behaviors of H_2O over the perfect Ni/TiO_2 (110) surface are similar to those on TiO_2(110), as shown in Fig. 10b. While in case of defect Ni/TiO_2(110) surface, the dissociation energy barrier of H_2O in oxygen vacancy is around 0.62–0.67 eV as shown in Figs 5 and 7, due to the stronger interaction of H_2O with the oxygen vacancy.

Adsorption of H_2O on Ni(111) surface was also investigated, which is very weak with the adsorption energy ranging from −0.02 to −0.25 eV. Meanwhile, a large dissociation energy barrier about 0.92 eV is needed to overcome, indicating that the steam adsorption and dissociation over Ni/TiO_2(110) surface can be mainly ascribed to the TiO_2(110) surface. Especially, the performance of TiO_2(110) surface on water adsorption and dissociation is better than YSZ and CeO_2 surfaces which are the traditional components of SOFC anode materials. As summarized in Table 1, the YSZ and CeO_2 surfaces are not as hydrophilic as TiO_2, and the dissociation energy barrier of H_2O on CeO_2 surface is about 2.35 eV. This result can also give a good explanation to the experimental observation that Ni/YSZ and Ni/SDC anodes are not so well carbon-tolerant as Ni/TiO_2 under open circuit condition even when exposed to humid methane fuels.

CONCLUSIONS

Based on the DFT calculations, we studied CO and H_2 formation on the Ni/TiO_2(110) surface. We found that

carbon reacting with interfacial TiO_2 lattice oxygen (C-O-steam path) was the dominating pathway, indicating that interfacial lattice oxygen played an active role in the formation of CO*. H_2O could obviously reduce the reaction energy of the whole reaction and thus make the CO and H_2 formation much more favorable in thermodynamics. Moreover, instead of serving as an oxidant, H_2O is much more readily to adsorbing and dissociating on the TiO_2 surface to wipe off the oxygen vacancies. In comparison with traditional anode materials, such as YSZ, CeO_2 and Ni, we found that TiO_2 greatly enhanced the adsorption and dissociation of H_2O on the surface which promoted the formation of CO as a result. And therefore, TiO_2 activated the adsorption and dissociation of H_2O to continuously provide interfacial oxygen as oxidant for the carbon conversion to CO.

Received 16 August 2019; accepted 13 November 2019; published online 16 December 2019

1 Barreto L, Makihira A, Riahi K. The hydrogen economy in the 21st century: A sustainable development scenario. Int J Hydrogen Energy, 2003, 28: 267–284
2 Sehested J. Four challenges for nickel steam-reforming catalysts. Catal Today, 2006, 111: 103–110
3 Bengaard HS, Nørskov JK, Sehested J, *et al.* Steam reforming and graphite formation on Ni catalysts. J Catal, 2002, 209: 365–384
4 Besenbacher F, Chorkendorff I, Clausen BS, *et al.* Design of a surface alloy catalyst for steam reforming. Science, 1998, 279: 1913–1915
5 Lin Y, Zhan Z, Liu J, *et al.* Direct operation of solid oxide fuel cells with methane fuel. Solid State Ion, 2005, 176: 1827–1835
6 Park S, Vohs JM, Gorte RJ. Direct oxidation of hydrocarbons in a solid-oxide fuel cell. Nature, 2000, 404: 265–267
7 Jung S, Lu C, He H, *et al.* Influence of composition and Cu impregnation method on the performance of Cu/CeO_2/YSZ SOFC anodes. J Power Sources, 2006, 154: 42–50
8 Tao , Irvine JTS. Catalytic properties of the perovskite oxide $La_{0.75}Sr_{0.25}Cr_{0.5}Fe_{0.5}O_{3-\delta}$ in relation to its potential as a solid oxide fuel cell anode material. Chem Mater, 2004, 16: 4116–4121
9 Tao S, Irvine JTS. A redox-stable efficient anode for solid-oxide fuel cells. Nat Mater, 2003, 2: 320–323
10 Ma Q, Tietz F. Comparison of Y and La-substituted $SrTiO_3$ as the anode materials for SOFCs. Solid State Ion, 2012, 225: 108–112
11 Marina O. Thermal, electrical, and electrocatalytical properties of lanthanum-doped strontium titanate. Solid State Ion, 2002, 149: 21–28
12 Suthirakun S, Ammal SC, Muñoz-García AB, *et al.* Theoretical investigation of H_2 oxidation on the $Sr_2Fe_{1.5}Mo_{0.5}O_6$ (001) perovskite surface under anodic solid oxide fuel cell conditions. J Am Chem Soc, 2014, 136: 8374–8386
13 Liu Q, Dong X, Xiao G, *et al.* A novel electrode material for symmetrical SOFCs. Adv Mater, 2010, 22: 5478–5482
14 Yang C, Yang Z, Jin C, *et al.* Sulfur-tolerant redox-reversible anode material for direct hydrocarbon solid oxide fuel cells. Adv Mater, 2012, 24: 1439–1443
15 Chen XJ, Khor KA, Chan SH. Suppression of carbon deposition at CeO_2-modified Ni/YSZ anodes in weakly humidified CH_4 at 850°C. Electrochem Solid-State Lett, 2005, 8: A79
16 Yang L, Choi YM, Qin W, *et al.* Promotion of water-mediated carbon removal by nanostructured barium oxide/nickel interfaces in solid oxide fuel cells. Nat Commun, 2011, 2: 357
17 Zhan Z, Barnett SA. An octane-fueled solid oxide fuel cell. Science, 2005, 308: 844–847
18 Shinde VM, Madras G. Catalytic performance of highly dispersed Ni/TiO_2 for dry and steam reforming of methane. RSC Adv, 2014, 4: 4817
19 Belhadi A, Trari M, Rabia C, *et al.* Methane steam reforming on supported nickel based catalysts. Effect of oxide ZrO_2, LaO_3 and nickel composition. Open J Phys Chem, 2013, 03: 89–96
20 Wang Z, Wang Z, Yang W, *et al.* Carbon-tolerant solid oxide fuel cells using $NiTiO_3$ as an anode internal reforming layer. J Power Sources, 2014, 255: 404–409
21 Ling Y, Wang Z, Wang Z, *et al.* A robust carbon tolerant anode for solid oxide fuel cells. Sci China Mater, 2015, 58: 204–212
22 Burghgraef H, Jansen APJ, van Santen RA. Electronic structure calculations and dynamics of methane activation on nickel and cobalt. J Chem Phys, 1994, 101: 11012–11020
23 Watwe RM, Bengaard HS, Rostrup-Nielsen JR, *et al.* Theoretical studies of stability and reactivity of CH_x species on Ni(111). J Catal, 2000, 189: 16–30
24 Jones G, Jakobsen J, Shim S, *et al.* First principles calculations and experimental insight into methane steam reforming over transition metal catalysts. J Catal, 2008, 259: 147–160
25 Au CT, Ng CF, Liao MS. Methane dissociation and syngas formation on Ru, Os, Rh, Ir, Pd, Pt, Cu, Ag, and Au: A theoretical study. J Catal, 1999, 185: 12–22
26 Zhang CJ, Hu P. Methane transformation to carbon and hydrogen on Pd(100): Pathways and energetics from density functional theory calculations. J Chem Phys, 2002, 116: 322
27 Huang ZQ, Long B, Chang CR. A theoretical study on the catalytic role of water in methanol steam reforming on PdZn(111). Catal Sci Technol, 2015, 5: 2935–2944
28 Ciobică IM, Frechard F, van Santen RA, *et al.* A theoretical study of CH_x chemisorption on the Ru(0001) surface. Chem Phys Lett, 1999, 311: 185–192
29 Ciobica IM, van Santen RA. A DFT study of CH_x chemisorption and transition states for C−H activation on the Ru(1120) surface. J Phys Chem B, 2002, 106: 6200–6205
30 Blöchl PE. Projector augmented-wave method. Phys Rev B, 1994, 50: 17953–17979
31 Kresse G, Hafner J. *Ab initio* molecular dynamics for open-shell transition metals. Phys Rev B, 1993, 48: 13115–13118
32 Kresse G, Furthmüller J. Efficient iterative schemes for *ab initio* total-energy calculations using a plane-wave basis set. Phys Rev B, 1996, 54: 11169–11186
33 Perdew JP, Burke K, Ernzerhof M. Generalized gradient approximation made simple. Phys Rev Lett, 1996, 77: 3865–3868
34 Monkhorst HJ, Pack JD. Special points for brillouin-zone integrations. Phys Rev B, 1976, 13: 5188–5192
35 Henkelman G, Uberuaga BP, Jónsson H. A climbing image nudged elastic band method for finding saddle points and minimum energy paths. J Chem Phys, 2000, 113: 9901–9904
36 Tait RH, Kasowski RV. Ultraviolet photoemission and low-energy-electron diffraction studies of TiO_2 (rutile) (001) and (110) surfaces. Phys Rev B, 1979, 20: 5178–5191
37 Ammal SC, Heyden A. Nature of Pt_n/TiO_2 (110) interface under water-gas shift reaction conditions: A constrained *ab initio* ther-

modynamics study. J Phys Chem C, 2011, 115: 19246–19259
38 Ammal SC, Heyden A. Origin of the unique activity of Pt/TiO_2 catalysts for the water–gas shift reaction. J Catal, 2013, 306: 78–90
39 Ammal SC, Heyden A. Water–gas shift catalysis at corner atoms of Pt clusters in contact with a TiO_2(110) support surface. ACS Catal, 2014, 4: 3654–3662
40 Li L, Zeng XC. Direct simulation evidence of generation of oxygen vacancies at the golden cage Au_{16} and TiO_2 (110) interface for CO oxidation. J Am Chem Soc, 2014, 136: 15857–15860
41 Chou JP, Hsing CR, Wei CM, *et al. Ab initio* random structure search for 13-atom clusters of fcc elements. J Phys-Condens Matter, 2013, 25: 125305
42 Blaylock DW, Ogura T, Green WH, *et al.* Computational investigation of thermochemistry and kinetics of steam methane reforming on Ni(111) under realistic conditions. J Phys Chem C, 2009, 113: 4898–4908
43 Zhu YA, Chen D, Zhou XG, *et al.* DFT studies of dry reforming of methane on Ni catalyst. Catal Today, 2009, 148: 260–267
44 Blaylock DW, Zhu YA, Green WH. Computational investigation of the thermochemistry and kinetics of steam methane reforming over a multi-faceted nickel catalyst. Top Catal, 2011, 54: 828–844
45 Kho ET, Scott J, Amal R. Ni/TiO_2 for low temperature steam reforming of methane. Chem Eng Sci, 2016, 140: 161–170
46 Rodriguez JA, Ma S, Liu P, *et al.* Activity of CeO_x and TiO_x nanoparticles grown on Au(111) in the water-gas shift reaction. Science, 2007, 318: 1757–1760
47 Hong S, Rahman TS. Rationale for the higher reactivity of interfacial sites in methanol decomposition on Au_{13}/TiO_2(110). J Am Chem Soc, 2013, 135: 7629–7635
48 Huang Y, Ling C, Jin M, *et al.* Water adsorption and dissociation on Ni surface: Effects of steps, dopants, coverage and self-aggregation. Phys Chem Chem Phys, 2013, 15: 17804–17817
49 Fronzi M, Piccinin S, Delley B, *et al.* Water adsorption on the stoichiometric and reduced CeO_2(111) surface: A first-principles investigation. Phys Chem Chem Phys, 2009, 11: 9188–9199

Acknowledgements This work was financially supported by the National Basic Research Program of China (2017YFA0402800 and 2016YFA0200602), the National Natural Science Foundation of China (51472228 and 21573204), the Fundamental Research Funds for the Central Universities (WK3430000004), and the One Hundred Person Project of CAS. The authors acknowledge the Supercomputing Center of the University of Science and Technology of China and the National Supercomputing Center in Tianjin for providing computational resources. Figures with geometry are based on the Jmol package (Jmol: an open-source Java viewer for chemical structures in 3D. http://www.jmol.org/).

Author contributions Yang W designed and performed the calculations, analyzed the data, and wrote the paper; Wang Z helped build the computational models; Tan W made contributions to Fig. 9 in the manuscript; Peng R, Wu X and Lu Y conceived the framework of this paper and revised the paper. All authors contributed to the general discussion.

Conflict of interest The authors declare that they have no conflict of interest.

Supplementary information The energy diagram of other CH-OH-steam path and CH-O-steam path and oxygen vacancy formation and migration path are available in the online version of the paper.

Wenqiang Yang was born in Sichuan, China. He received his bachelor's (2012) and master's (2015) degrees in materials science from Nanjing University of Science and Technology and the University of Science and technology of China (USTC), respectively. He is now a PhD student at Andreas Heyden's group at University of South Carolina. His current research focuses on computational heterogeneous catalysis and machine learning application on catalysis.

Ranran Peng received her PhD degree in materials science from the USTC in 2003. She currently is an associate professor in USTC. Her scientific interests include exploring novel electrode materials and revealing electrode reaction mechanisms for solid oxide fuel cells, and developing fantastic spintronic and multiferroic materials.

Yalin Lu was born in Jiangsu, China. He received his PhD from Nanjing University in 1991, and is now a full professor in USTC. Before joining USTC, he was a professor in AFA, Tufts University and Lawrence Berkeley National Laboratory. He currently serves as the Director of National Synchrotron Radiation Laboratory of China. His research focuses on quantum functional materials, nanophotonics, new energy materials and THz technologies.

Ni/TiO_2(110)表面甲烷重整反应生成CO和H_2反应机理的第一性原理研究

杨文强[1], 王振斌[1], 谭文周[1], 彭冉冉[1*], 武晓君[1,2,3*], 陆亚林[1,2,3*]

摘要 基于密度泛函理论(DFT)计算，本文研究了Ni/TiO_2(110)表面甲烷重整反应的机理，揭示了固体氧化物燃料电池中TiO_2基阳极较传统ZrO_2或者CeO_2基阳极材料具有良好抗积碳性能的重要原因. 本文对六种不同的甲烷重整反应路径(干燥和湿润的气氛环境)进行了详细研究，阐明了TiO_2, Ni/TiO_2界面和水分子在甲烷重整反应中的作用以及Ni/TiO_2基阳极抗积碳性能的来源. 经过计算发现，在干燥和湿润的环境下，碳原子和界面的TiO_2晶格氧反应生成CO，以及后续水分子吸附和解离在界面的氧空位上并提供反应所需O原子是甲烷重整反应的主要路径(C-O路径)，而水分子直接参与C原子或者CH基团的氧化反应则要困难很多. 值得注意的是，在研究的六种反应路径中，CO从反应表面的脱附都非常困难，需要约2.3 eV的能量才能使得其脱附. 因而造成大量表面反应活性位点被占据，这是目前很多阳极材料不具备抗积碳性能的一个重要原因. 然而，在湿润环境中，水分子的吸附放热大大降低了整个反应体系所需能量，尤其是本文中水分子在TiO_2表面的快速解离吸附更是大大降低了整个反应体系的能量. 进一步研究发现，水分子在Ni, YSZ和CeO_2表面的吸附解离要比在TiO_2表面困难很多. 这也是TiO_2基阳极材料具有较好抗积碳性能的一个重要原因. 本研究对于指导合成碳氢燃料气氛下具有优异抗积碳性能的固体氧化物燃料电池阳极材料具有重要的意义.

